Spectrochimica Acta Part A 78 (2011) 926–934

Contents lists available at ScienceDirect

Spectrochimica Acta Part A: Molecular and Biomolecular Spectroscopy

journal homepage: www.elsevier.com/locate/saa

Versatile binding properties of a di-2-pyridyl ketone nicotinoylhydrazone ligand: Crystal structure of a Cu(II) complex

Neema Ani Mangalam, M.R. Prathapachandra Kurup*

Department of Applied Chemistry, Cochin University of Science and Technology, Kochi, Kerala 682 022, India

ARTICLE INFO

Article history:
Received 6 January 2010
Received in revised form 27 October 2010
Accepted 30 November 2010

Keywords:
Hydrazones
Crystal structure
Di-2-pyridyl ketone
Copper(II) complexes
ESR spectra

ABSTRACT

Six new copper complexes of di-2-pyridyl ketone nicotinoylhydrazone (HDKN) have been synthesized. The complexes have been characterized by a variety of spectroscopic techniques and the structure of $[Cu(DKN)_2]\cdot H_2O$ has been determined by single crystal X-ray diffraction. The compound $[Cu(DKN)_2]\cdot H_2O$ crystallized in the monoclinic space group $P2_1$ and has a distorted octahedral geometry. The IR spectra revealed the presence of variable modes of chelation for the investigated ligand. The EPR spectra of compounds $[Cu_2(DKN)_2(\mu\text{-}N_3)_2]$ and $[Cu_2(DKN)_2(\mu\text{-}NCS)_2]$ in polycrystalline state suggest a dimeric structure as they exhibited a half field signal, which indicate the presence of a weak interaction between two Cu(II) ions in these complexes.

1. Introduction

Acid hydrazides and their corresponding products, heteroaroylhydrazones, have attracted much attention in synthetic chemistry and inorganic chemistry due to their use in biological systems and analytical chemistry. Due to the chelating behavior, they are used in analytical chemistry as selective metal extracting agents as well as in spectroscopic determination of certain metals [1]. Mixed ligand metal complexes of hydrazones, have proved to be useful catalysts in reactions such as hydrogenation, oxidation, carbonylation and hydroformylation [2]. The applications of rhenium–carbonyl compounds as electrochemical sensors and the optosensing behavior of ruthenium(II), manganese(I) compounds of di-2-pyridyl ketone have been reported [3,4]. The use of these systems as molecular sensors is due to their high values of extinction coefficients and low values for their activation parameters. Interest in these ligands has been driven, in part, by potentially beneficial biological activity of the ligands and the metal complexes, including antimicrobial, antitumor, anti-convulsant, anti-inflammatory and antibacterial [5,6]. Some hydrazone analogues namely di-2-pyridyl ketone isonicotinoylhydrazone were found to effectively promote the efflux of intracellular Fe and inhibit the uptake of Fe from transferrin by tumor cells in culture [7]. Moreover they have been investigated as promising agents for the treatment of neoplasia and were suggested as potential oral chelating drugs for the treatment of genetic disorders such as thalassemia [8].

Recently we have reported the synthesis and characterization of some new hydrazones and their vanadium complexes [9]. We have been interested in the chemistry of polypyridyl containing ligands and as an extension of our previous work [9] we have used di-2-pyridyl ketone nicotinoylhydrazone as a precursor to synthesize and characterize a series of Cu(II) complexes. Di-2-pyridyl ketone nicotinoylhydrazone is an interesting synthon in the class of chelating agents. These ligands exhibit keto-enol tautomerism and can coordinate metal ions in neutral and monoanionic forms [10–12]. The choice of di-2-pyridyl ketone is mainly due to the fact that this heteroaromatic moiety can provide a further binding site for metal cations [13,14]. It is rigid, and provides two aromatic nitrogens whose unshared electron pairs are beautifully placed to act co-operatively in binding cations. Thus it seemed interesting to investigate the coordinating behavior of the ligand, and in this paper we report the spectral and structural aspects of some newly synthesized copper(II) complexes.

2. Experimental

2.1. Materials

Di-2-pyridyl ketone (Aldrich), nicotinic hydrazide (Aldrich), copper(II) chloride dihydrate (E-Merck), copper(II) acetate monohydrate (E-Merck), sodium azide (Reidel-De Haen), potassium thiocyanate (Merck), copper(II) bromide (Aldrich), copper(II) perchlorate hexahydrate (Aldrich) were used as supplied

---

* Corresponding author. Tel.: +91 484 2862423; fax: +91 484 2575804.
E-mail address: mrp@cusat.ac.in (M.R. Prathapachandra Kurup).

1386-1425/$ – see front matter © 2010 Elsevier B.V. All rights reserved.
doi:10.1016/j.saa.2010.11.032

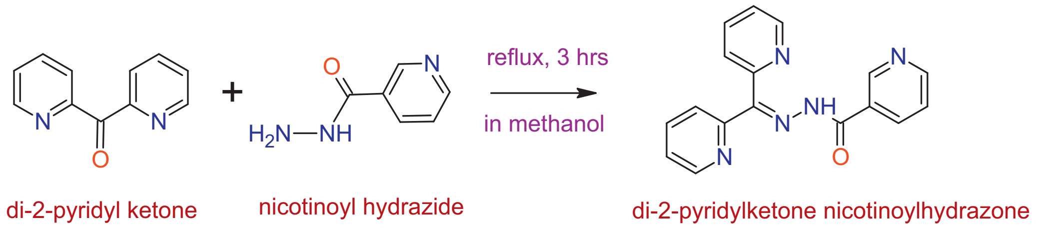

Scheme 1. Synthesis of di-2-pyridyl ketone nicotinoyl hydrazone.

and solvents were purified by standard procedures before use.

2.2. Synthesis of di-2-pyridyl ketone nicotinoylhydrazone hemihydrate (HDKN·0.5H_2O)

The ligand di-2-pyridyl ketone nicotinoylhydrazone hemihydrate (HDKN·0.5H_2O) was prepared as reported by us earlier [9]. To a methanolic solution of nicotinoyl hydrazide (0.137 g, 1 mmol), di-2-pyridyl ketone (0.184 g, 1 mmol) in methanol was added. The reaction mixture was refluxed for 5 h and was kept at room temperature for slow evaporation. After a week, a white compound was separated, filtered and washed with ether and dried over P_4O_{10} *in vacuo*. Yield: 84%, Color: colorless, M.P.: 159 °C, Elemental *Anal.* Found (Calcd.) (%): C: 65.94 (65.37), H: 4.26 (4.52), N: 22.47 (22.42) for HDKN·0.5H_2O. Selected IR (cm^{-1}) bands: ν(N–H) 2928 w; ν(C=O) 1689 vs; ν(C=N) 1579 s.

Electronic absorption bands (MeCN) λ_{max} (nm): 223, 269, 318 (Scheme 1).

2.3. Syntheses of complexes

2.3.1. Synthesis of [Cu(DKN)$_2$] (**1**)

Complex **1** was prepared by refluxing a methanolic solution of HDKN·0.5H_2O (1 mmol, 0.312 g) and $Cu(CH_3COO)_2 \cdot H_2O$ (1 mmol, 0.199 g) for 5 h. The resulting solution was allowed to stand at room temperature and after slow evaporation, dark green crystalline compound was separated, filtered and washed with ether and dried over P_4O_{10} *in vacuo*.

[Cu(DKN)$_2$] (**1**): Yield: 81%, λ_m (DMF): 5 Ω^{-1} cm^2 mol^{-1}, μ_{eff} (B.M.): 1.72, Elemental *Anal.* Found (Calcd.) (%): C: 60.86 (61.12), H: 3.58 (3.62), N: 20.36 (20.96).

2.3.2. Syntheses of [Cu(HDKN)Cl_2] (**2**), [Cu(DKN)Br] (**3**) and [Cu_2(DKN)$_2$](ClO_4)$_2$·2H_2O (**4**)

Complexes **2**, **3** and **4** were prepared by refluxing equimolar methanolic solutions of HDKN with corresponding copper salt solutions. The resulting solution was allowed to stand at room temperature and after slow evaporation, the green products were separated, filtered and washed with ether and dried over P_4O_{10} *in vacuo*.

[Cu(HDKN)Cl_2] (**2**): Yield: 75%, λ_m (DMF): 9 Ω^{-1} cm^2 mol^{-1}, μ_{eff} (B.M.): 1.89, Elemental *Anal.* Found (Calcd.) (%): C: 46.56 (46.64), H: 2.67 (2.99), N: 15.56 (16.00).

[Cu(DKN)Br] (**3**): Yield: 78%, λ_m (DMF): 12 Ω^{-1} cm^2 mol^{-1}, μ_{eff} (B.M.): 1.86, Elemental *Anal.* Found (Calcd.) (%): C: 45.26 (45.81), H: 2.96 (2.71), N: 15.20 (15.71).

[Cu_2(DKN)$_2$](ClO_4)$_2$·2H_2O (**4**): Yield: 90%, λ_m (DMF): 165 Ω^{-1} cm^2 mol^{-1}, μ_{eff} (B.M.): 1.26, Elemental *Anal.* Found (Calcd.) (%): C: 42.38 (42.25), H: 2.99 (2.92), N: 14.61 (14.49).

2.3.3. Synthesis of [Cu_2(DKN)$_2$(μ-N_3)$_2$] (**5**)

Complex **5** was prepared by stirring methanolic solution of HDKN (1 mmol, 0.312 g) and aqueous solution of NaN_3 (1 mmol, 0.065 g) for half an hour and then $Cu(CH_3COO)_2 \cdot H_2O$ (1 mmol, 0.199 g) in distilled water was added to the mixture and again stirred for 2 h. Green precipitate obtained was filtered, washed with methanol and dried over P_4O_{10} *in vacuo*.

[Cu_2(DKN)$_2$(μ-N_3)$_2$] (**5**): Yield: 85%, λ_m (DMF): 8 Ω^{-1} cm^2 mol^{-1}, μ_{eff} (B.M.): 1.24, Elemental *Anal.* Found (Calcd.) (%): C: 49.73 (50.06), H: 2.40 (2.97), N: 27.68 (27.47).

2.3.4. Synthesis of [Cu_2(DKN)$_2$(μ-NCS)$_2$] (**6**)

Complex **6** was prepared in a similar manner as complex **5** by using KSCN instead of NaN_3. Green crystalline complex obtained was filtered, washed with methanol and dried over P_4O_{10} *in vacuo*.

[Cu_2(DKN)$_2$(μ-NCS)$_2$] (**6**): Yield: 70%, λ_m (DMF): 3 Ω^{-1} cm^2 mol^{-1}, μ_{eff} (B.M.): 1.42, Elemental *Anal.* Found (Calcd.) (%): C: 50.55 (51.00), H: 2.31 (2.85), N: 19.82 (19.82).

Caution! Although no problems were encountered during this research, azide and perchlorate salts of metal complexes with organic ligands are potentially explosive. So they should be prepared in small quantities and handled with care.

2.4. Physical measurements

C, H and N analyses of the ligand and the complexes were performed on a Vario EL III CHNS analyzer at SAIF, Kochi, India. The IR spectra were recorded on a JASCO FT/IR-4100 Fourier Transform Infrared spectrometer using KBr pellets in the range 400–4000 cm^{-1}. Electronic spectra in acetonitrile solutions were recorded on a Spectro UV–vis Double Beam UVD-3500 spectrometer in the 200–900 nm range. The molar conductances of the complexes in DMF (10^{-3} M) solutions were measured at 298 K with a Systronic model 303 direct-reading conductivity bridge. Magnetic susceptibility measurements at 298 K were made using a MSB mk1 magnetic susceptibility balance from Sherwood Scientific Limited. EPR spectra of complexes in solid state at 298 K and in frozen DMF at 77 K were recorded on a Varian E-112 spectrometer at X-band, using TCNE as standard with 100 kHz modulation frequency and 9.1 GHz microwave frequency at SAIF, IIT Bombay, India.

2.5. X-ray crystallography

X-ray quality crystals of [Cu(DKN)$_2$]·H_2O (**1a**) were grown from a solution of **1** in methanol-acetonitrile mixture. Hydrogen atoms of water could not be located and were not included in the model. The determination of the crystal structure was carried out on a Bruker P4 X-ray diffractometer using graphite monochromated Mo Kα radiation (λ = 0.71073 Å) at 153 K. The data were solved using Bruker SHELXTL by direct method and refined by the full matrix least squares method on F^2 using Bruker SHELXTL [15]. The Bruker SAINT software was used for data reduction and Bruker SMART for cell refinement. The atoms C(32) and C(33) of a pyridine ring are disordered over two sites with relative occupancies of 58 and 42% for A and B components respectively. All non-hydrogen atoms were refined with anisotropic displacement parameters. The hydrogen atoms attached to carbons were placed in calculated positions with

Table 1
Crystal data and structure refinement parameters for complex **1a**.

Parameters	$[Cu((DKN)_2]\cdot H_2O$ (**1a**)
Empirical formula	$C_{34}H_{24}CuN_{10}O_3$
Formula weight (M)	684.18
Temperature (*T*) (K)	153(2) K
Wavelength (Mo Kα) (Å)	0.71073
Crystal system	Monoclinic
Space group	$P2_1$
Lattice constants	
a (Å)	9.3770(19)
b (Å)	10.111(2)
c (Å)	16.763(3)
α (°)	90
β (°)	101.33(3)
γ (°)	90
Volume (*V*) ($Å^3$)	1557.2(5)
Z	2
Calculated density (ρ) ($Mg\,m^{-3}$)	1.459
Absorption coefficient (μ) (mm^{-1})	0.755
F(000)	702.0
Crystal size (mm^3)	0.28 × 0.28 × 0.38
θ range for data collection	2.22–25.00°
Limiting indices	$-11 \le h \le 11$ $-12 \le k \le 12$ $-19 \le l \le 19$
Reflections collected	14,918
Unique reflections	5466
Refinement method	Full-matrix least-squares on F^2
Data/restraints/parameters	5086/17/453
Goodness-of-fit on F^2	1.055
Final *R* indices [$I > 2\sigma(I)$]	$R_1 = 0.0356$, $wR_2 = 0.086$
R indices (all data)	$R_1 = 0.0387$, $wR_2 = 0.0875$

$wR_2 = \left[\sum w(F_o^2 - F_c^2)^2 / \sum w(F_o^2)^2\right]^{1/2}$.
$R_1 = \Sigma||F_o| - |F_c|| / \Sigma|F_o|$.

C–H = 0.93 Å (aromatic protons) and $U(H) = 1.2\,U_{eq}$ (C) and refined isotropically in the riding model approximation. Molecular structure of the compound was created using the ORTEP program [16] and packing diagram was plotted using MERCURY [17]. Pertinent crystallographic data and structure refinement parameters for the structure are given in Table 1.

3. Results and discussion

The syntheses of all complexes were straight forward and high yielding. The compounds are soluble in organic solvents such as CH_3CN, DMSO and DMF. The analytical and spectroscopic data are in good agreement with the chemical formulas of the complexes. The ligand and its Cu(II) complexes are very stable at room temperature and remain for a long time without decomposition. The molar conductance values of all the compounds except **4** are in the range 3–12 $\Omega^{-1}\,cm^2\,mol^{-1}$, indicating their non-electrolytic nature, but **4** is found to be a 2:1 electrolyte [18]. Magnetic moments for the complexes were calculated from magnetic susceptibility measurements using diamagnetic corrections. Mononuclear Cu(II) complexes exhibit magnetic moments in the range 1.7–1.9 B.M., which corresponds to a single unpaired electron [19]. The low magnetic moment for the dinuclear complexes may be attributed to the presence of antiferromagnetic spin–spin interaction. From the spectroscopic characterization, it is found that di-2-pyridyl ketone nicotinoylhydrazone acts as a tridentate ligand coordinating through azomethine, one of the pyridyl nitrogens and enolate oxygen *via* deprotonation which was also evident from the crystal structure of complex **1a**.

3.1. Crystal structure of $[Cu(DKN)_2]\cdot H_2O$ (**1a**)

A view of the Cu(II) complex with the atom numbering scheme is presented in Fig. 1 as an ORTEP plot [16]. Selected interatomic distances and bond angles are provided in Table 2. The Cu(II) ion is in an N_4O_2 coordination sphere in which each of the two meridionally spanning ligands coordinates the metal ion *via* the pyridine-N, imine-N and deprotonated amide-O atoms forming two five membered chelate rings [20]. A distinguishing feature of Cu(II) structure is its asymmetry. In similar complexes reported containing Mn(II), Ni(II) and Zn(II) divalent metal ions, the pairs of corresponding coordinate bond lengths to the two ligands are more or less the same, but here the two ligands bonded to copper are distinct [21]. One ligand forms Cu–N and Cu–O bond lengths that are consistently longer than those of the other ligand. The distortion forcing

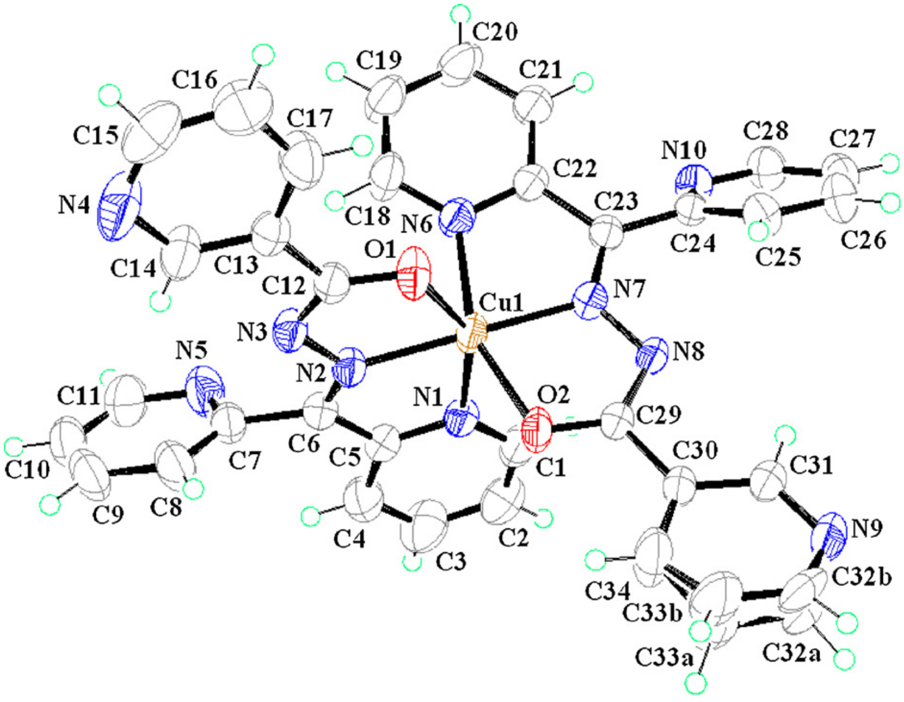

Fig. 1. The molecular structure of $[Cu(DKN)_2]\cdot H_2O$ (**1a**) along with the atom numbering scheme.

Table 2
Selected bond lengths (Å) and bond angles (°) for $[Cu(DKN)_2]\cdot H_2O$.

Bond lengths	Bond angles
Cu1–N2 1.986(2)	N2–Cu1–N7 171.7(3)
Cu1–N7 1.947(2)	N2–Cu1–O1 74.8 (6)
Cu1–O1 2.253(2)	N2–Cu1–N1 76.3 (9)
Cu1–O2 2.066(2)	N7–Cu1–O2 78.2 (5)
Cu1–N1 2.276(3)	N7–Cu1–N6 79.0 (0)
Cu1–N6 2.069(2)	O1–Cu1–N1 150.9(8)
N2–N3 1.378(3)	O2–Cu1–N6 156.1(9)
N7–N8 1.357(3)	N7–Cu1–N1 96.7(9)
N2–C6 1.299(4)	N2–Cu1–N6 97.2(9)
N7–C23 1.297(3)	N6–Cu1–N1 99.2(2)
O1–C12 1.253(3)	O2–Cu1–N1 90.3(4)
O2–C29 1.264(3)	N6–Cu1–O1 88.2(8)
N3–C12 1.338(4)	N2–Cu1–O2 106.1(7)
N8–C29 1.338(4)	O2–Cu1–O1 93.8(7)
	C6–N2–N3 118.1(2)
	C23–N7–N8 122.3(2)

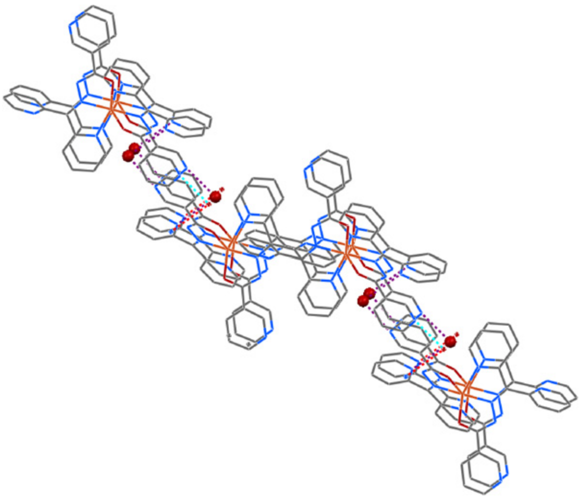

Fig. 2. Packing diagram of $[Cu(DKN)_2]\cdot H_2O$ along 'b' axis.

O1 and N2 away from the Cu ion is so large that Cu–N3 bond is also weakened. The deviation from perfect octahedron is evident from the bond distances and angles given in Table 2. For e.g. the ideally linear trans angle N3–Cu1–N8 is ~172.11(14)° and the interligand angle N2–Cu1–O1 is ~150.75(12)°, which gives clear evidence for the deviation from perfect octahedron [22]. Least square analyses shows that planes containing O1, N2, N1, Cu1 and N7 (plane 1) and O2, N7, N6, Cu1 and N2 (plane 2) shows a maximum deviation from the mean plane of −1.3274(5) Å for N1 and 1.1553(4) Å for N6 and the dihedral angle formed by the two planes is 49.07(1)°.

There is one lattice water per molecule and the hydrogen bonding interactions are shown in Table 3. Thus adjacent molecules are linked into chains by these interactions as shown in Fig. 2. The metal chelate ring Cg(8) {N6, C18, C19, C20, C21, C22} is stacked *via* π–π interactions with Cg(9) {N9, C30, C31, C32A, C33A, C34} of the neighboring unit with a centroid to centroid distance of 3.708(5) Å [23]. In addition to the π–π stacking, significant C–H···π interactions of the pyridyl hydrogens with metal chelate rings of the neighboring molecules adds the stability of the unit cell packing (Table 3). Ring puckering analyses shows that two five membered rings Cg(1) {Cu1–O1–C12–N3–N2}, Cg(2) {Cu1–O2–C29–N8–N7} are puckered [24] and adopts an envelope conformation on Cu1 (Q(2) = 0.145(2) Å, Phi(2) = 360.0(11)°) and twisted conformation on N7 (Q(2) = 0.1042(19) Å, Phi(2) = 350.0(14)°) respectively.

3.2. Infrared spectra

The significant IR frequencies of the ligand are given in the experimental section. Bonding of the hydrazone to Cu(II) center has been suggested by a careful comparison of the infrared spectra of the complexes with that of the free ligand. The main stretching frequencies of the IR spectra of the complexes and their tentative assignments are tabulated in Table 4. The ν(NH) and ν(C=O) stretching bands at 2928 and 1689 cm^{-1} respectively, corresponding to the free ligand are not observed in the spectra of the complexes [25,26]. This fact, along with the presence of a medium intensity band at *ca.* 1369 cm^{-1} assignable to ν(C–O), indicates that the hydrogen atoms of the amide group are lost during the synthesis and the deprotonated ligand is predominantly in the enolate form in the complexes [27]. But in complex **2**, the ligand is coordinated in the keto form which is evident from its spectrum with a peak at 1604 cm^{-1} due to ν(C=O) band. A very strong and sharp band located at 1579 cm^{-1} is assigned to the ν(C=N) stretching vibrations of azomethine of the ligand. This band is shifted to lower wavenumber on complexation with the metal [28], which supports the participation of azomethine group of the ligand in binding to the Cu(II) ion and is consistent with the X-ray diffraction studies

Table 3
H-bonding, π–π and C–H···π interaction parameters of $[Cu(DKN)_2]\cdot H_2O$.

H-bonding						
D – H···A (Å)	D – H	H···A	D···A	D – H···A		
C1–H(1)···N(9)[a]	0.93	2.62	3.371(4)	138		
C10–H(10)···O(2)[b]	0.93	2.50	3.221(4)	135		
C20–H(20)···N(9)[c]	0.93	2.58	3.389(5)	145		
Equivalent position code *a* = 2 − *x*, 1/2 + *y*, 1 − *z*, *b* = 1 − *x*, 1/2 + *y*, −*z*, *c* = 1 − *x*, 1/2 + *y*, 1 − *z*, π–π interactions						
Cg(I)···Cg(J)	Cg–Cg (Å)	α (°)	β (°)	γ (°)	CgI_Perp	CgJ_Perp
Cg(8)···Cg(9)[d]	3.708(5)	5.6(4)	24.77	19.33	3.4986(14)	−3.367(4)
Cg(9)···Cg(8)[e]	3.708(5)	5.6(4)	19.33	24.77	−3.366(4)	3.4986(14)
Equivalent position code *d* = −1 + *x*, *y*, *z*, *e* = 1 + *x*, *y*, *z*						
			Cg(8) = N(6), C(18), C(19), C(20), C(21), C(22); Cg(9) = N(9), C(30), C(31), C(32A), C(33A), C(34)			
C–H···π interaction						
X – H···Cg(J)	H···Cg (Å)		X – H···Cg (°)		X···Cg (Å)	
C(28)–H(28)···Cg(2)[f]	2.64		150		3.482(3)	
Equivalent position code *f* = 1 − *x*, 1/2 + *y*, 1 − *z*			Cg(2) = Cu (1), O(2), C(29), N(8), N(7)			

D, donor; A, acceptor; Cg, centroid; α, dihedral angles between planes I and J; β, angle Cg(I) – Cg(J) vector normal to plane I; γ, angle Cg(I) – Cg(J) vector normal to plane J; CgI_Perp, perpendicular distance of Cg(I) on ring J; CgJ_Perp, perpendicular distance of Cg(J) on ring I.

Table 4
Infrared spectral data (cm^{-1}) of the copper(II) complexes.

Compound	ν(C=N)	ν(C=N)^a	ν(C=O)/ν(C–O)	ν(N–N)	ν(Cu–N$_{azo}$)	ν(Cu–O)
[Cu(DKN)$_2$] (**1**)	1521 (m)	1585 (s)	1351 (m)	1075 (m)	471 (w)	433 (w)
[Cu(HDKN)Cl$_2$] (**2**)	1509 (s)	–	1604 (s)	1082 (m)	483 (w)	443 (w)
[Cu(DKN)Br] (**3**)	1501 (s)	1583 (m)	1371 (s)	1086 (m)	477 (w)	447 (w)
[Cu$_2$(DKN)$_2$](ClO$_4$)$_2$·2H$_2$O (**4**)	1505 (s)	1590 (m)	1382 (s)	1083 (m)	467 (w)	430 (w)
[Cu$_2$(DKN)$_2$(μ-N$_3$)$_2$] (**5**)	1506 (m)	1585 (m)	1375 (s)	1090 (m)	464 (w)	442 (w)
[Cu$_2$(DKN)$_2$(μ-NCS)$_2$] (**6**)	1503 (s)	1582 (m)	1368 (s)	1082 (m)	463 (w)	441 (w)

s, strong; m, medium and w, weak.
[a] Newly formed C=N.

in complex **1a**. A shift to the higher frequency of the ν(N–N) band and the appearance of a new band due to ν(C=N) may be taken as additional evidence for the participation of the imine nitrogen [28]. This new band is absent in complex **2**, since the ligand is coordinating in the keto form. The low energy pyridine ring in-plane and out-of-plane vibrations observed in the spectrum of the ligand at 615 cm^{-1}, are shifted to higher frequencies in the case of complexes, which is a good indication of the coordination of the heterocyclic nitrogen to the metal center [29].

In the perchlorate complex, bands corresponding to ν(NH) and ν(C=O) stretching are absent and a new band is observed at 1382 cm^{-1} which suggests the hydrazone has coordinated to the metal in the enolate form. Also the azomethine stretching has undergone shift to lower wavenumbers together with the appearance of a new band at 1590 cm^{-1} which may be due to the formation of new (C=N) bond. This gives the evidence for the coordination of azomethine nitrogen. In addition to this, a strong absorption at 1091 cm^{-1} [30] and an unsplit band at 623 cm^{-1}, indicates the presence of ionic perchlorate group. This was also evident from the molar conductivity measurements. The most interesting part of the spectra in complexes **5** and **6** is the 2000–2100 cm^{-1} region where the strong absorption bands due to the azide and thiocyanate group are visible. The azido bridges in complex **5** take the end-on structure with the ν_a(N$_3$) at 2057 cm^{-1} [31]. In **5** and **6**, the azomethine band has undergone downward shift to 1506 and 1503 cm^{-1} respectively thus suggesting the coordination through azomethine nitrogen. Also the ν(NH) and ν(C=O) bands are absent and the ν(C–O) stretching vibrations are observed at 1375 and 1368 cm^{-1} respectively which indicates that the hydrazone has undergone deprotonation and has coordinated in the enolate form. In complex **6**, a single strong and sharp peak at 2078 cm^{-1}, assignable to ν(CN) stretching mode of thiocyanate group is observed which corresponds to the bridging CN stretching [31]. The pyridyl nitrogen coordination in **4**, **5** and **6** complexes are evident from the shifting of out-of-plane bending modes of vibrations of the free ligand at 622 cm^{-1} to higher energies.

3.3. Electronic spectra

The absorption bands of the ligand are discussed in the experimental section and that of the complexes are listed in Table 5. For the Cu(II) complexes with an elongated tetragonally distorted octahedral crystal field symmetry or in square planar geometry of D$_{4h}$ symmetry, three spin allowed transitions are expected *viz.* $^2A_{1g} \leftarrow {}^2B_{1g}$, $^2B_{2g} \leftarrow {}^2B_{1g}$, $^2E_g \leftarrow {}^2B_{1g}$ which occur in the ranges 850–550, 645–555 and 580–500 nm, respectively [32]. But often these theoretical expectations are unseen in practice and these bands usually appear overlapped and become difficult to resolve into separate bands due to the very small energy difference between the *d* levels. The presence of a broad band in all the complexes in the range 660–700 nm can be assigned to the envelope of $^2A_{1g} \leftarrow {}^2B_{1g}$, $^2B_{2g} \leftarrow {}^2B_{1g}$, $^2E_g \leftarrow {}^2B_{1g}$ transitions. The intense bands observed at ~390 nm in all Cu(II) complexes are mainly due to the phenoxy O → Cu(II) charge transfer transitions [33,34]. The remaining bands of the complexes ~260 and 280 nm correspond to the intraligand π–π^* and n–π^* transitions which suffered marginal shifts when compared to that of the free ligand.

Table 5
Electronic spectral data of the copper(II) complexes.

Compound	UV–vis absorption bands (nm)
[Cu(DKN)$_2$] (**1**)	253, 273 (sh), 388, 699
[Cu(HDKN)Cl$_2$] (**2**)	258, 296 (sh), 399, 664
[Cu(DKN)Br] (**3**)	253, 278 (sh), 397, 683
[Cu$_2$(DKN)$_2$](ClO$_4$)$_2$·2H$_2$O (**4**)	253, 276 (sh), 393, 669
[Cu$_2$(DKN)$_2$(μ-N$_3$)$_2$] (**5**)	251, 273 (sh), 397, 664
[Cu$_2$(DKN)$_2$(μ-NCS)$_2$] (**6**)	253, 275 (sh), 395, 686

3.4. EPR spectra

For the case of a 3d^9 copper(II) ion, the appropriate spin Hamiltonian assuming a B$_{1g}$ ground state is given by

$$\hat{H} = \beta[g_{||}B_zS_z + g_{\perp}(H_xS_x + H_yS_y)]_{+}A_{||}I_zS_z + A_{\perp}(I_xS_x + I_yS_y)$$

The EPR spectra of all the compounds were recorded in polycrystalline state at 298 K and in frozen DMF at 77 K in the X band frequency and various magnetic induction parameters are summarized in Table 6. EPR spectra of **2**, **3** and **4** in frozen DMF were not good and were rerecorded in DMSO. The experimental and simulated best fits [35] of EPR spectra of some of the complexes in DMF/DMSO at 77 K are given in Fig. 3. The polycrystalline state spectra of all the compounds except [Cu$_2$(DKN)$_2$](ClO$_4$)$_2$·3H$_2$O and [Cu$_2$(DKN)$_2$(μ-NCS)$_2$] were axial in nature. The geometric parameter *G*, and the bonding parameters of all the spectra are calculated. For axial spectra, *G* which is a measure of the exchange interactions between the copper centers, is calculated using the equation: $G = (g_{||} - 2.0023)/(g_{\perp} - 2.0023)$. If $G < 4.0$ considerable exchange interaction is indicated in the solid complex [36,37]. The value of in-plane sigma bonding parameter α^2 was estimated for each species, from the expression [38],

$$\alpha^2 = -\frac{A_{||}}{0.036} + (g_{||} - 2.0023) + \frac{3}{7}(g_{\perp} - 2.0023) + 0.04.$$

The orbital reduction factors $K_{||}$ and $K_{\perp}$ were estimated from the expression

$$K_{||} = \frac{(g_{||} - 2.0023)E_{d-d}}{8\lambda_o}$$

$$K_{\perp} = \frac{(g_{\perp} - 2.0023)E_{d-d}}{2\lambda_o}$$

where $K_{||} = \alpha^2\beta^2$, $K_{\perp} = \alpha^2\gamma^2$ and λ_o represent the one electron spin–orbit coupling constant for the free ion, equal to –828 cm^{-1}. Significant information about the nature of bonding in the copper(II) complexes can be derived from the magnitude of $K_{||}$ and $K_{\perp}$. In case of pure σ bonding $K_{||} \approx K_{\perp} \approx 0.77$ whereas $K_{||} < K_{\perp}$ implies

Table 6
EPR spectral assignments of copper(II) complexes in polycrystalline state and in frozen DMF at 77 K.

	1	2	3	4	5	6
Polycrystalline (298 K)						
$g_{\|\|}/g_1$	2.352	2.198	2.138	2.044	2.244	2.053
$g_{\perp}/g_2, g_3$	2.108	2.106	2.110	2.110, 2.198	2.059	2.069, 2.244
g_{iso}/g_{av}	2.189	2.136	2.119	–	2.120	–
G	3.308	1.887	1.259	–	4.262	–
DMF (77 K)						
$g_{\|\|}/g_1$	2.015	2.192	2.060	–	2.225	2.270
$g_{\perp}/g_2, g_3$	2.086, 2.248	2.079	2.142	–	2.055	2.040
g_{av}/g_{iso}	–	2.116	2.114	2.110	2.111	2.116
$A_{\|\|}$	111.36[a]	–	–	–	165.50[a]	166.02[a]
α^2	–	–	–	–	0.742	0.784
β^2	–	–	–	–	0.940	0.975
γ^2	–	–	–	–	0.911	0.728
$K_{\|\|}$	–	–	–	–	0.698	0.765
$K_{\perp}$	–	–	–	–	0.677	0.571

[a] Expressed in units of cm^{-1} multiplied by a factor of 10^{-4}.

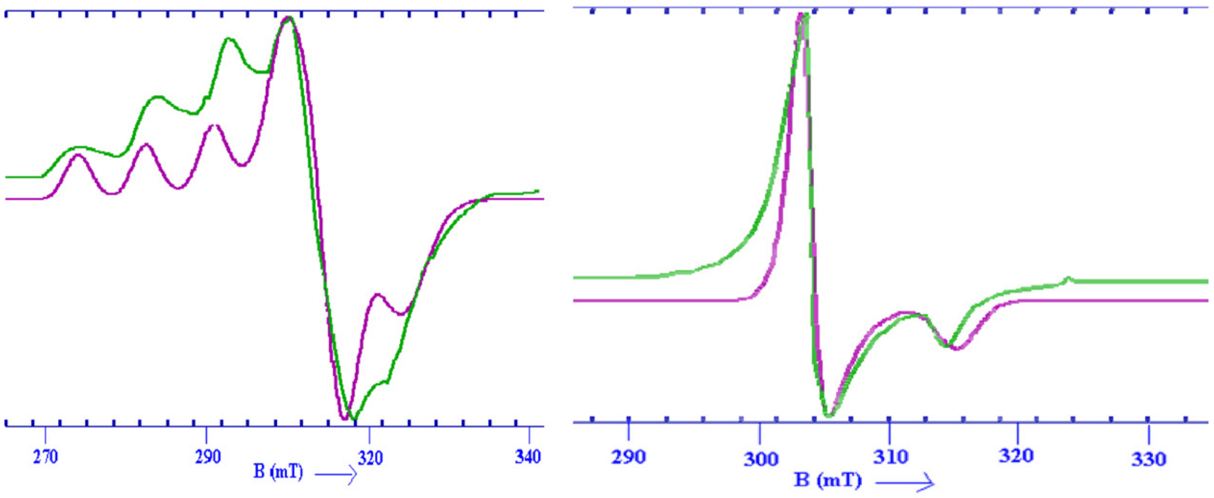

[Cu(DKN)$_2$] (**1**) [Cu(DKN)Br] (**3**)

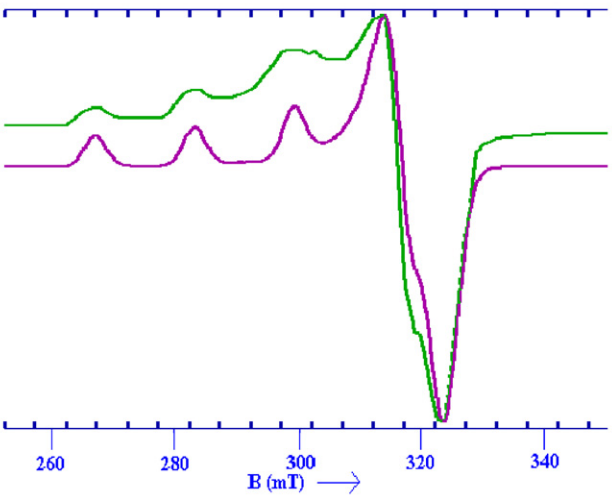

[Cu$_2$(DKN)$_2$(μ-N$_3$)$_2$] (**5**)

Fig. 3. Experimental (green) and simulated best fit (purple) of the EPR spectra of complexes **1**, **3** and **5** in frozen DMF at 77 K. (For interpretation of the references to color in this figure legend, the reader is referred to the web version of the article.)

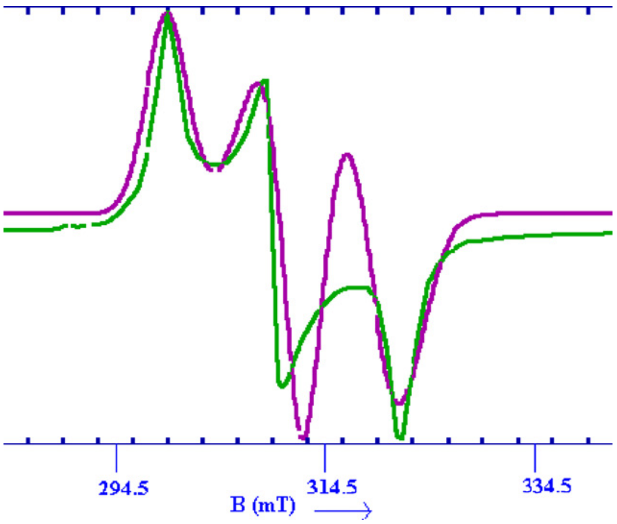

Fig. 4. EPR spectrum of $[Cu_2(DKN)_2](ClO_4)_2{\cdot}2H_2O$ in polycrystalline state at 298 K. (For interpretation of the references to color in this figure legend, the reader is referred to the web version of the article.).

considerable in-plane bonding, while for out-of-plane bonding, $K_{||} > K_{\perp}$.

The EPR parameters $g_{||}$, $g_{\perp}$, $A_{||}$(Cu) and energies of d–d transitions were used to evaluate the bonding parameters α^2, β^2 and γ^2, which may be regarded as a measure of covalency of the in-plane σ-bonds, in-plane π-bonds and out-of-plane π-bonds respectively [39]. Since α^2 values decreases with increasing covalency and obtained values lies above 0.5 and below 1.0, it is inferred that the complexes have significant covalent character in the ligand environment.

EPR spectra of polycrystalline samples of compounds **1**, **2**, **3** and **5** are axial in nature even though the hyperfine splittings were not very clear since it is magnetically concentrated but the perchlorate and thiocyanate derivatives undergo distortion around the metal center and the lower symmetry is reflected in the rhombic spectra obtained for these complexes (Fig. 4). Three g values g_1, g_2, g_3 were observed and the large anisotropy in these values is indicative of a geometry distorted from regular octahedron in the solid state. In polynuclear Cu(II) complexes the most important application of the measurement of the EPR spectra is in the identification of Cu–Cu dipolar interaction. Additional transitions arise associated with the $\Delta M_s = \pm 2$ values, compared with the $\Delta M_s = \pm 1$ values in mononuclear complexes. In the X-band spectra, $\Delta M_s = \pm 1$ transitions are associated with fields of *ca.* 300 mT, while the $\Delta M_s = \pm 2$ generate an absorption at the half field value of *ca.* 150 mT and the presence of this half field band is a useful criterion for dipolar interaction for the presence of some dinuclear or polynuclear complex formation [40]. The EPR spectra of compounds **5** and **6** in polycrystalline state suggest a dimeric structure as they exhibited a half field signal at 146.5 and 158 mT, respectively (Fig. 5), which indicate that indeed a weak interaction between two Cu(II) ions is present in these compounds. But the absence of a signal at half field corresponding to $\Delta M_s = \pm 2$ forbidden transition in complex **4** indicates that the exchange interaction is very weak.

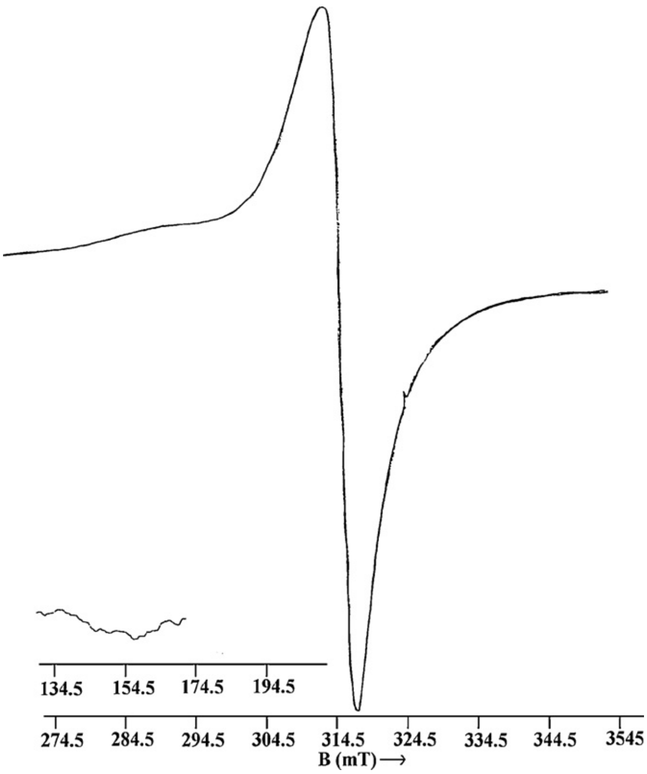

Fig. 5. EPR spectrum of $[Cu_2(DKN)_2(\mu\text{-}N_3)_2]$ in polycrystalline state at 298 K.

In frozen DMF at 77 K, the spectrum of compound **1** is found to be rhombic in nature with three g values g_1, g_2, g_3, where $g_3 > g_2 > g_1$

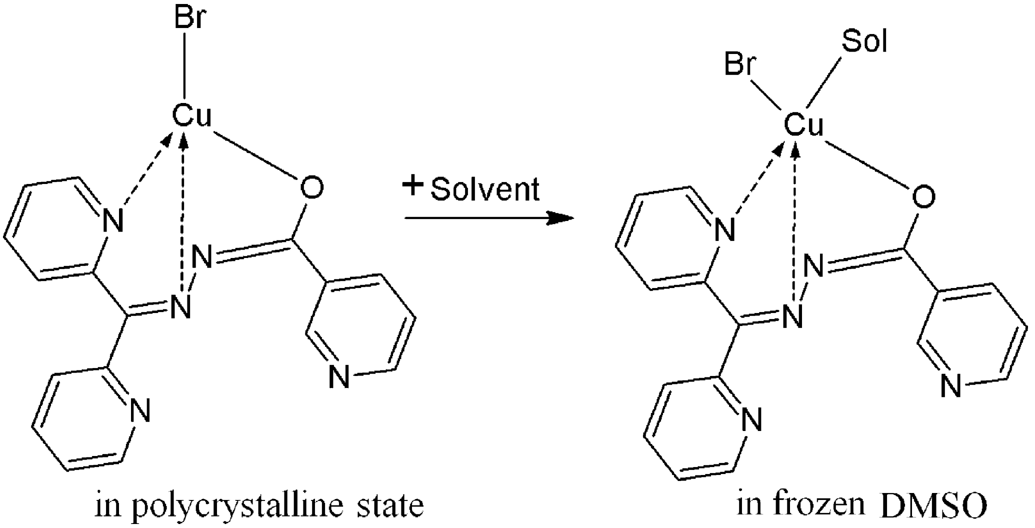

Fig. 6. Change in the coordination of **3** in DMSO.

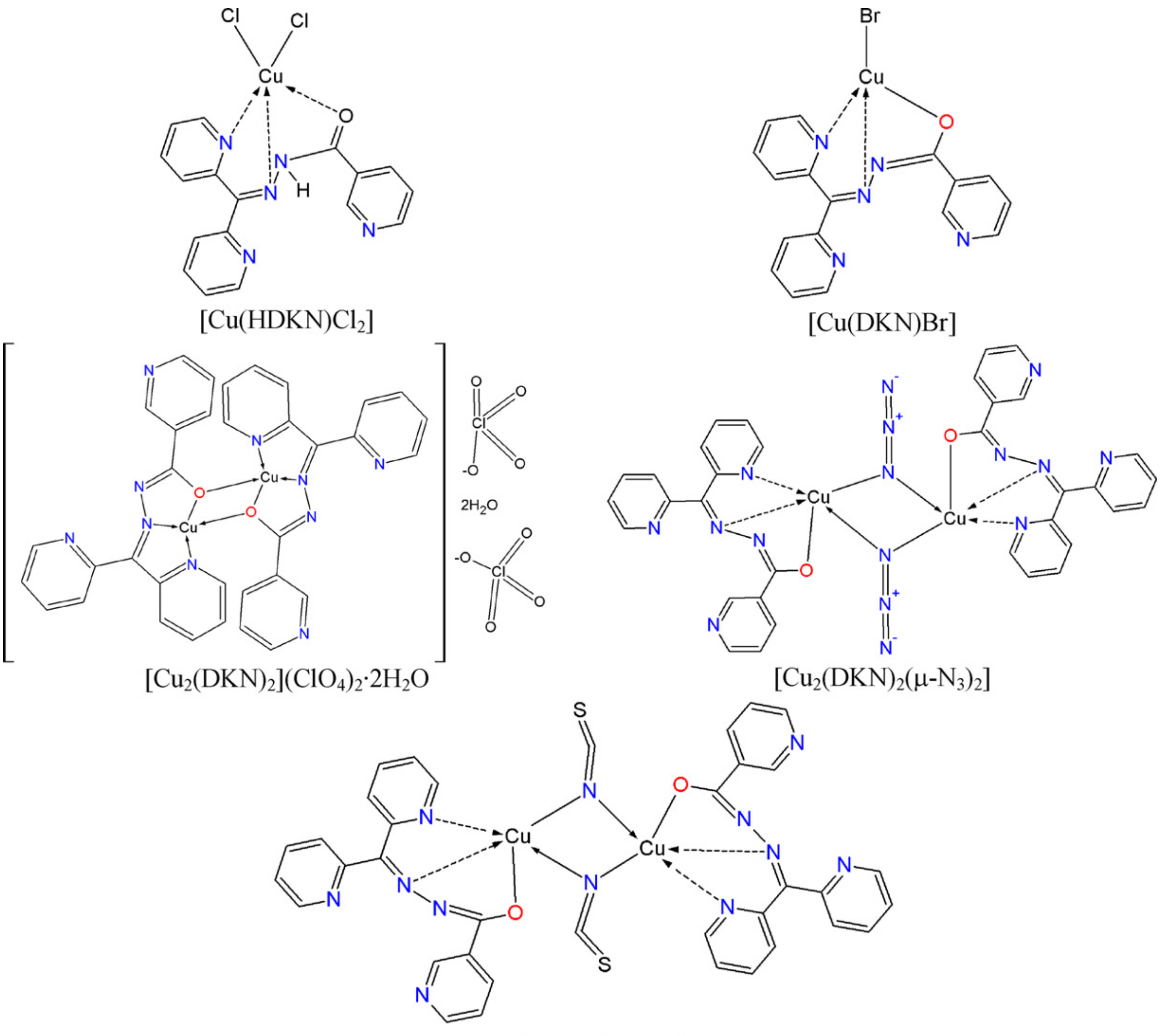

$[Cu(HDKN)Cl_2]$

$[Cu(DKN)Br]$

$[Cu_2(DKN)_2](ClO_4)_2{\cdot}2H_2O$

$[Cu_2(DKN)_2(\mu\text{-}N_3)_2]$

$[Cu_2(DKN)_2(\mu\text{-}NCS)_2]$

Fig. 7. Proposed structures of the synthesized complexes.

and four hyperfine splittings are observed in the parallel region as evidenced in the spectrum (Fig. 3). The spectrum of **2** is broad but not isotropic in nature and does not give much information, but even more dramatic changes occur in the powder ESR spectrum of compound **3** from an axial spectrum at room temperature to a reverse axial spectrum in DMSO at 77 K. These changes correspond with the variations of stereochemistry from square planar to trigonal bipyramidal structure which may be due to the coordination of the solvent (Fig. 6) with $g_\perp > g_{||} > 2.0023$ relationship with a d_z^2 ground state [41]. DMSO is an aggressive solvent, so solvolysis of the complex and a change in coordination geometry in that solvent is not unreasonable. The spectrum of compound **4** does not show any anisotropic feature and hyperfine splittings, which may be due to poor glass formation, while **5** and **6** were found to be axial in nature with four hyperfine splittings due to the coupling of the electron spin with the nuclear spin of ^{63}Cu ($I = 3/2$) with different $g_{||}$ and $g_\perp$ values consistent with a $d_{x^2-y^2}$ ground state with an elongated octahedral geometry [42,43].

4. Conclusions

From the above observations it was found that di-2-pyridyl ketone nicotinoylhydrazone could coordinate to the metal center either in the neutral or in deprotonated form. Some of the complexes were found to be dimeric in nature which was evident from EPR spectra. The perchlorate compound was found to be ionic in nature which was evident from the molar conductivity value. In all the complexes the hydrazone was found to coordinate to Cu(II) center through the pyridyl, azomethine nitrogens and the amide oxygen either in neutral or deprotonated form. Based on the above observations proposed structures of the synthesized complexes are shown in Fig. 7.

Supplementary data

Crystallographic data for the structural analysis has been deposited with the Cambridge Crystallographic Data Center, CCDC 695749 for compound $[Cu(DKN)_2]{\cdot}H_2O$. The data can be obtained free of charge at www.ccdc.cam.ac.uk/conts/retrieving.html [or from Cambridge Crystallographic Data Centre (CCDC), 12 Union Road, Cambridge CB21EZ, UK; fax: +44 1223 336 033; e-mail: deposit@ccdc.cam.ac.uk].

Acknowledgements

M.R.P. Kurup is thankful to KSCSTE, Thiruvananthapuram, India for financial assistance and N.A. Mangalam thanks Cochin University of Science and Technology for the award of SRF. The authors are thankful to the SAIF, Cochin University of Science and Technology, Kochi, Kerala, India for elemental analyses and IR spectra. We are thankful to IIT Bombay, India for EPR spectra. We are thankful to Prof. M.V. Rajasekharan, School of Chemistry, University of Hyderabad for providing single crystal XRD data and EPR simulation package.

Appendix A. Supplementary data

Supplementary data associated with this article can be found, in the online version, at doi:10.1016/j.saa.2010.11.032.

References

[1] M. Bakir, C. Gyles, J. Mol. Struct. 649 (2003) 133–142.
[2] M. De Gui, R.-H. Zhang, H. Yan, H.-M. Wang, X.-B. Chen, S.-J. Zhu, Synth. React. Inorg. Met. – Org. Chem. 28 (1998) 1381–1391.
[3] M. Bakir, O. Green, C. Gyles, Inorg. Chim. Acta 358 (2005) 1835–1840.
[4] M. Bakir, O. Green, C. Gyles, Spectrochim. Acta Part A 72 (2009) 50–55.
[5] W. Luo, X.-G. meng, G.-Z. Cheng, Z-P. Ji, Inorg. Chim. Acta 362 (2009) 551–555.
[6] N. Ozbek, G. Kavak, Y. Ozcan, S. Ide, N. Karacan, J. Mol. Struct. 919 (2009) 154–159.
[7] P.V. Bernhardt, G.J. Wilson, P.C. Sharpe, D.S. Kalinowski, R. Des, Richardson, J. Biol. Inorg. Chem. 13 (2008) 107–119.
[8] E.M. Becker, D.B. Lovejoy, J.M. Greer, R.N. Watts, D.R. Richardson, Br. J. Pharmacol. 138 (2003) 819–830.
[9] N.A. Mangalam, S. Sivakumar, S.R. Sheeja, M.R.P. Kurup, E.R.T. Tiekink, Inorg. Chim. Acta 362 (2009) 4191–4197.
[10] R.N. Patel, K.K. Shukla, A. Singh, M. Choudhary, U.K. Chauhan, S. Dwivedi, Inorg. Chim. Acta 362 (2009) 4891–4898.
[11] A.A.R. Despaigne, J.G. Da Silva, A.C.M. Do Carmo, O.E. Piro, E.E. Castellano, H. Beraldo, J. Mol. Struct. 920 (2009) 97–102.
[12] N.R. Sangeetha, S. Pal, Polyhedron 19 (2000) 1593–1600.
[13] O. Pouralimardan, A.-C. Chamayou, C. Janiak, H.H. Monfared, Inorg. Chim. Acta 360 (2007) 1599–1608.
[14] T.A. Reena, E.B. Seena, M.R.P. Kurup, Polyhedron 27 (2008) 1825–1831.
[15] G.M. Sheldrick, SHELXTL98, Version 5. 1, Bruker AXS, Inc., Madison, Wisconsin, USA, 1999.
[16] L.J. Farrugia, J. Appl. Crystallogr. 30 (1997) 565–1565.
[17] C.F. Macrac, P.R. Edington, P. McCabe, E. Pidcock, G.P. Shields, R. Taylor, M. Towler, J. Van de Streek, J. Appl. Crystallogr. 39 (2006) 453–457.
[18] W.J. Geary, Coord. Chem. Rev. 7 (1971) 109–111.
[19] N. Filipovic, H. Borrmann, T. Todorovic, M. Borna, V. Spasojevic, D. Sladic, I. Novakovic, K. Andjelkovic, Inorg. Chim. Acta 362 (2009) 1996–2000.
[20] M. Sebastian, V. Arun, P.P. Robinson, P. Leeju, D. Varghese, G. Varsha, K.K.M. Yusuff, J. Coord. Chem. 63 (2010) 307–314.
[21] A.S. Pedrares, N. Camina, J. Romero, M.L. Duran, J.A.G. Vazquez, A. Sousa, Polyhedron 27 (2008) 3391–3397.
[22] A.R. Stefankiewicz, M.W. -Chorab, H.B. Szczesniak, V. Patroniak, M. Kubicki, Z. Hnatejko, J. Harrowfield, Polyhedron 29 (2010) 178–187.
[23] M. Kuriakose, M.R.P. Kurup, Struct. Chem. 18 (2007) 579–584.
[24] D. Cremer, J.A. Pople, J. Am. Chem. Soc. 97 (1975) 1354–1358.
[25] R.M. Issa, A.A. Hassanein, I.M. El-Mehasseb, R.I.A. El-Wadoud, Spectrochim. Acta Part A 65 (2006) 206–214.
[26] M.F. Iskander, T.E. Khalil, R. Werer, W. Haase, I. Svoboda, H. Fuess, Polyhedron 19 (2000) 949–958.
[27] R.C. Maurya, S. Rajput, J. Mol. Struct. 833 (2007) 133–144.
[28] H. Yin, Acta Crystallogr. C 64 (2008) 324–326.
[29] A. Ray, S. Banerjee, R.J. Butcher, C. Desplanches, S. Mitra, Polyhedron 27 (2008) 2409–2415.
[30] V. Philip, V. Suni, M.R.P. Kurup, M. Nethaji, Polyhedron 24 (2005) 1133–1142.
[31] K. Nakamoto, Infrared and Raman Spectra of Inorganic and Coordination compounds, 5th ed., Wiley, New York, 1997.
[32] A.B.P. Lever, Inorganic Electronic Spectroscopy, 2nd ed., Elsevier, Amsterdam, 1984.
[33] M. Singh, V. Aggarwal, U.P. Singh, N.K. Singh, Polyhedron 28 (2009) 195–199.
[34] G.S. Siluvai, N.N. Murthy, Polyhedron 28 (2009) 2149–2156.
[35] G. Swarnabala, M.V. Rajasekharan, Inorg. Chem. 28 (1989) 662–666.
[36] S.A. El-Enein, F.A. El-Saied, S.M. Emam, M.A. Ell-Salamony, Spectrochim. Acta Part A 71 (2008) 421–429.
[37] I.M. Procter, B.J. Hathaway, P. Nicholls, J. Chem. Soc. A (1968) 1678–1684.
[38] M. Antosik, N.M.D. Brown, A.A. McConnell, A.L. Porte, J. Chem. Soc. A (1969) 545–550.
[39] U.L. Kala, S. Suma, S. Krishnan, M.R.P. Kurup, R.P. John, Polyhedron 26 (2007) 1427–1435.
[40] N.F. Albanese, H.M. Haendler, Polyhedron 2 (1983) 1131–1140.
[41] I.M. Procter, F.S. Stephens, J. Chem. Soc. A (1969) 1248–1255.
[42] V.P. Singh, Spectrochim. Acta Part A 71 (2008) 17–22.
[43] S. Verma, S. Chandra, U. Dev, N. Joshi, E. Garribba, S. Mitra, Spectrochim. Acta Part A 74 (2009) 370–374.